Available online at www.sciencedirect.com

SCIENCE DIRECT®

ELSEVIER

Journal of Catalysis 232 (2005) 143–151

JOURNAL OF CATALYSIS

www.elsevier.com/locate/jcat

Dehydrogenation of propane to propene over different polymorphs of gallium oxide

Bo Zheng, Weiming Hua, Yinghong Yue [*], Zi Gao

Department of Chemistry and Shanghai Key Laboratory of Molecular Catalysis and Innovative Materials, Fudan University, Shanghai 200433, P.R. China

Received 23 December 2004; revised 23 February 2005; accepted 1 March 2005

Abstract

Dehydrogenation of propane to propene in the presence or absence of CO_2 over four polymorphs of gallium oxide was investigated. β-Ga_2O_3 exhibits the highest activity among the polymorphs, and it is even more active than chromium oxide catalyst in the presence of CO_2. H_2-TPR and XPS studies show that gallium oxide is hardly reduced below 600 °C. The dehydrogenation reaction is suggested to proceed through a heterolytic dissociation reaction pathway, and it is enhanced by CO_2 because of the existence of the reverse water gas shift reaction and the Boudouard reaction. The high catalytic activity of β-Ga_2O_3 is probably associated with an abundance of surface medium-strong acid sites related to the coordinatively unsaturated Ga^{3+} cations and the conjugated effect of proton and oxide. Furthermore, increasing the reaction temperature facilitates the activation of CO_2 over β-Ga_2O_3. The promoting effect of CO_2 on β-Ga_2O_3 catalyst is more evident above 550 °C.

Keywords: Gallium oxide; Propane; Dehydrogenation; Carbon dioxide; Reaction mechanism

1. Introduction

The process of catalytic dehydrogenation of alkanes into their corresponding alkenes is of increasing importance because of the growing demand for alkenes. Propene is an important raw material for the production of polypropene, polyacrylonitrile, acrolein, and acrylic acid. Dehydrogenation of propane is an endothermic reaction that requires relatively high temperature to obtain a high yield of propene. The high reaction temperature favours thermal cracking reactions to coke and light alkanes, leading to a decrease in product yield and an increase in catalyst deactivation. Hence, the oxidative dehydrogenation of propane by oxygen has been proposed as an alternative to the process. The latter is an exothermic reaction, which is an advantage from the engineering and economic viewpoints. However, the selectivity of the catalytic reaction is still an unsolved problem. The overoxidation of propane to carbon dioxide in the reaction is unavoidable. Recently, carbon dioxide has been utilized as an oxidant in several partial oxidation reactions, such as reforming and oxidative coupling of methane. The oxidative dehydrogenation of propane by carbon dioxide has also been reported to give rather high propene selectivity [1,2]. The promoting effect of carbon dioxide on the reaction has been observed on catalysts, such as silica-supported Cr_2O_3 [1], rare earth vanadates [3], and Ga_2O_3 [4]. Since carbon dioxide is one of the major greenhouse gases, the use of carbon dioxide is attractive not only economically but also ecologically.

Aromatization of light paraffins over Ga-promoted H-ZSM-5 catalysts has been studied intensely in the previous decade. There are different interpretations concerning the role of gallium in the aromatization reaction. Many authors agree that the aromatization reaction occurs via a bifunctional mechanism, and gallium enhances the dehydrogenation steps, including the dehydrogenation of alkane, higher olefins, and cycloolefins [5–10]. More recently, it has

---

[*] Corresponding author. Fax: +86 21 65641740.
E-mail address: yhyue@fudan.edu.cn (Y. Yue).

0021-9517/$ – see front matter © 2005 Elsevier Inc. All rights reserved.
doi:10.1016/j.jcat.2005.03.001

been found that carbon dioxide can markedly promote dehydrogenation of ethane and propane over gallium oxide or gallium-loaded catalysts [11–14]. The olefin yield is greatly increased in the presence of CO_2.

Gallium oxide has five polymorphs, designated α-, β-, γ-, δ-, and ε-Ga_2O_3 [15]. Of these, β-Ga_2O_3 is the stable form. All of these phases of gallium oxide except ε-Ga_2O_3 can be prepared under specific conditions [15,16]. In this work, the four polymorphs of gallium oxide (α-, β-, γ-, δ-Ga_2O_3) were prepared and characterized by X-ray diffraction (XRD), nitrogen adsorption at −196 °C, temperature-programmed desorption (TPD) of NH_3 and CO_2, temperature-programmed reduction (TPR), X-ray photoelectron spectroscopy (XPS), and ^{71}Ga MAS NMR spectroscopy. The catalytic performance of these polymorphs for dehydrogenation of propane to propene in the presence or absence of CO_2 was compared and discussed in relation to their physicochemical properties and the mechanism of the reaction.

2. Experimental

2.1. Catalyst preparation

α-, β-, and δ-Ga_2O_3 were prepared according to the procedures described in the literature [15]. α-Ga_2O_3 was synthesized by a precipitation method. Aqueous NH_3 solution (14 wt%) was added to a 10 wt% gallium nitrate ($Ga(NO_3)_3 \cdot xH_2O$; Aldrich) solution. The precipitate was dried at 100 °C and calcined in air at 500 °C for 6 h. β-Ga_2O_3 was prepared by thermal decomposition of $Ga(NO_3)_3 \cdot xH_2O$ at 600 °C for 6 h in air. $Ga(NO_3)_3 \cdot xH_2O$ was heated at 200 °C overnight to produce δ-Ga_2O_3, which was then calcined at 500 °C for 6 h in air. To prepare γ-Ga_2O_3 [16], $Ga(NO_3)_3 \cdot xH_2O$ was first dissolved in ethanol (approximately 3 g of the salt in 50 ml of the solvent); then an ethanol solution of aqueous ammonia (ethanol/aqueous NH_3 = 1:1) was slowly added with continuous stirring at room temperature until no further precipitate was formed. The resulting gel was filtered, washed with ethanol, and vacuum-dried in a desiccator. The xerogel thus obtained was calcined at 500 °C for 6 h to form γ-Ga_2O_3. Chromium oxide used in this work was prepared by thermal decomposition of $Cr(NO_3)_3 \cdot 9H_2O$ at 600 °C for 6 h in air.

2.2. Catalyst characterization

X-ray powder diffraction (XRD) was used to identify the crystal phases of gallium oxide catalysts before and after reaction. The measurements were carried out on a Rigaku D/Max-IIA diffractometer with Cu-K_α radiation at 30 kV and 20 mA, running from 15° to 70° with a speed of 8°/min. The specific surface areas of the catalysts were measured by nitrogen adsorption at −196 °C with a Micromeritics ASAP 2000 instrument and calculated by the BET method. The surface acidity was measured by NH_3 temperature-programmed desorption (NH_3-TPD) in a flow-type fixed-bed reactor at ambient pressure, and the surface basicity was measured by CO_2 temperature-programmed desorption (CO_2-TPD) with a similar apparatus. The sample (50 mg) was preheated at 500 °C for 3 h and cooled to 120 °C in flowing He. At this temperature, sufficient pulses of NH_3 or CO_2 were injected until adsorption saturation, followed by purging with He for about 2 h. The temperature was then raised from 120 to 500 °C at a rate of 10 °C/min to desorb NH_3 or CO_2 and was further maintained at 500 °C for 30 min. The NH_3 or CO_2 desorbed was collected in a liquid N_2 trap and detected by gas chromatography. Temperature-programmed reduction (TPR) experiments were carried out on a Micromeritics TPD/TPR 2900 instrument with 25 mg catalyst under a gas flow (40 ml/min) of hydrogen (10%) and argon (90%). The catalyst was pretreated in N_2 flow at 300 °C for 3 h. The temperature was increased from 50 to 500 °C at a ramp rate of 10 °C/min. A thermal conductivity detector was used to monitor the hydrogen consumed during the TPR course. CuO was used as a standard sample for the calibration of hydrogen consumption. Thermal gravimetric analysis (TGA) was conducted on a Perkin–Elmer TGA7 apparatus to determine the amount of coke deposited on the catalyst after the reaction. Twenty milligrams of sample was heated from room temperature to 550 °C at a heating rate of 10 °C/min in flowing air. The X-ray photoelectron spectra (XPS) were obtained with Al-K_α radiation (1486.6 eV) on a Perkin–Elmer PHI 5000C ESAC system at a base pressure of 1×10^{-9} Torr. The sample was pressed into a $\varnothing\ 13 \times 1$ mm round disc and was degassed in the pretreatment chamber for 2 h before being transferred to the analysis chamber for XPS measurement. All binding energy (BE) values were referenced to the C(1s) peak at 284.6 eV. ^{71}Ga MAS NMR measurements were performed on a Bruker Avance DMX-500 spectrometer operating at 152.5 MHz, equipped with a 2.5-mm double bearing MAS probehead spinning at 30 kHz. Approximately 60,000 transients were accumulated for α-Ga_2O_3 and 40,000 for β- and γ-Ga_2O_3 with a 0.1-s recycling delay. The chemical shifts were referenced to 1 mol/l $Ga(NO_3)_3$ solution.

2.3. Reaction testing

Catalytic tests were performed in a fixed-bed flow microreactor at atmospheric pressure, and the catalyst load was 200 mg. Nitrogen was used as the carrier gas at a flow rate of 10 ml/min. The catalysts were pretreated at 500 °C for 1 h in nitrogen flow, and the reaction temperature was 500 °C. For nonoxidative dehydrogenation of propane, the gas reactant contained 2.5 vol% propane and a balance of nitrogen. For oxidative dehydrogenation of propane by carbon dioxide, the gas reactant contained 2.5 vol% propane, 5 vol% carbon dioxide, and a balance of nitrogen.

The hydrocarbon reaction products were analyzed with an on-line gas chromatograph with a 6-m column of Porapak Q and a flame ionization detector (FID). The gas products, such as N_2, CO, and CO_2, were analyzed with another chromatograph equipped with a 2-m packed column of carbon molecular sieve 601 and a thermal conductance detector (TCD). The conversion and selectivity were calculated as follows:

$$\mathrm{C_3H_8\ conversion} = \frac{\mathrm{C_3H_{8\ in}} - \mathrm{C_3H_{8\ out}}}{\mathrm{C_3H_{8\ in}}} \times 100\%,$$

$$\mathrm{CO_2\ conversion} = \frac{\mathrm{CO_{2\ in}} - \mathrm{CO_{2\ out}}}{\mathrm{CO_{2\ in}}} \times 100\%,$$

$$\mathrm{C_3H_6\ selectivity} = \frac{\mathrm{C_3H_{6\ out}}}{\mathrm{C_3H_{8\ in}} - \mathrm{C_3H_{8\ out}}} \times 100\%.$$

The reaction data in the work were reproducible with a precision of less than 5%.

3. Results

3.1. Catalyst synthesis and structural identification

We prepared α-Ga_2O_3 by calcining $Ga(OH)_3$ gel in air at 500 °C for 6 h. The diffraction pattern of α-Ga_2O_3 obtained is shown in Fig. 1a. Only peaks at 24.5°, 33.5°, 36.2°, 41.2°, 50.2°, 55.4°, 63.4°, and 65.0°, corresponding to the diffractions of (102), (014), (110), (113), (204), (116), (124), and (330) of α-Ga_2O_3, are observed, showing that the sample is a pure α-Ga_2O_3. β-Ga_2O_3 is the only stable form of Ga_2O_3. It is possible to easily obtain β-Ga_2O_3 by heating any other form of Ga_2O_3 or its hydrate in air above 1000 °C or hydrothermally above 300 °C [15]. In the present work, $Ga(NO_3)_3$ was used as the precursor and was calcined in air at 600 °C for 6 h to get β-Ga_2O_3. The diffraction pattern of β-Ga_2O_3 is shown in Fig. 1b. The peaks at 30.1°, 30.5°, 31.7°, 33.5°, 35.2°, 37.5°, 38.4°, 43.0°, 45.8°, 48.7°, 49.6°, 54.6°, 57.5°, 60.0°, 60.8°, 62.7°, and 64.7°, corresponding to the diffractions of (004), $(10\bar{4})$, (200), $(11\bar{1})$, (111), (104), $(11\bar{3})$, (113,211), $(006,21\bar{1})$, (015), (204), (115,302), $(31\bar{3})$, (311), (020), (008,017,022), and $(12\bar{2}, 215)$ of β-Ga_2O_3, are observed. The pattern is very similar to that of the β-Ga_2O_3 sample prepared by calcining of γ-Ga_2O_3 at 800 °C for 4 h, described in the literature [17]. γ-Ga_2O_3 can be obtained by a precipitation method. In earlier literatures [15,18] gallia gel was prepared by the addition of ammonia to an aqueous solution of gallium nitrate. The filtered gel was quickly dried before calcination to prevent the formation of GaO(OH), which forms α- or β-Ga_2O_3 after calcination. The γ-Ga_2O_3 product obtained by this method contained other gallia polymorphs. Recently, Areán et al. [16] successfully prepared pure γ-Ga_2O_3 by using ethanol as a solvent instead of water, so the latter method was adopted in this work. The diffraction pattern of the sample prepared is shown in Fig. 1c. Only peaks at 30.8°, 36.2°, 44.1°, 58.2°, and 64.2°, corresponding to the diffractions of (220), (113), (004), (333,115), and (440) of γ-Ga_2O_3, respectively, are observed. $Ga(NO_3)_3$ was heated at 200 °C for about 12 h to produce δ-Ga_2O_3, which was then calcined at 500 °C for 6 h, since the temperature of propane dehydrogenation in this work is 500 °C. The diffraction pattern of δ-Ga_2O_3 is shown in Fig. 1d, in which only peaks at 31.2°, 35.9°, and 61.8°, corresponding to the diffractions of (222), (400), and (622) of δ-Ga_2O_3, respectively, are observed, showing that δ-Ga_2O_3 is formed. It has been reported [15] that when δ-Ga_2O_3 is heated at 525 °C it transforms into ε-Ga_2O_3 within 30 min. We have tried to prepare ε-Ga_2O_3 from δ-Ga_2O_3 but failed because of its instability, so the catalytic test for ε-Ga_2O_3 is not included in the present work.

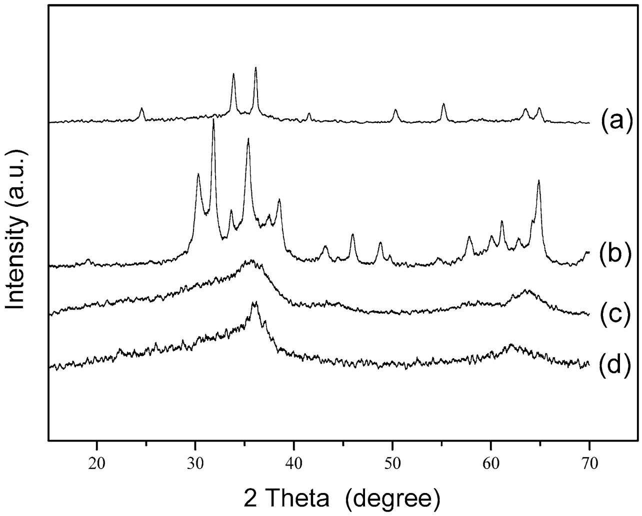

Fig. 1. XRD patterns of fresh gallium oxide catalysts. (a) α-Ga_2O_3; (b) β-Ga_2O_3; (c) γ-Ga_2O_3; (d) δ-Ga_2O_3.

3.2. Dehydrogenation of propane

Dehydrogenation of propane over different polymorphs of gallium oxide in the absence of CO_2 was studied at 500 °C; the results are given in Table 1 and Fig. 2. The major product formed in the reaction is propene, and the minor products are ethane, ethylene, and methane. It is interesting to note that the gallium oxides behave differently in the reaction. The initial conversion of propane on the catalysts decreases in the order γ-Ga_2O_3 > β-Ga_2O_3 > δ-Ga_2O_3 > α-Ga_2O_3. For all of the catalysts, the propane conversion drops gradually with reaction time and almost reaches steady state after 6 h. The steady-state conversion of propane for the catalysts is in the order γ-Ga_2O_3 > α-Ga_2O_3, β-Ga_2O_3 > δ-Ga_2O_3. Since the gallium oxides differ considerably in specific surface area, the specific activities of the oxides (expressed in terms of $\mu mol/(h\,m^2)$) were calculated. Intrinsically, β-Ga_2O_3 is almost twice as active as the other gallium oxide catalysts, both initially and at steady state.

At the beginning of the reaction, the selectivity for propene on the catalysts is about 85–95%. α-Ga_2O_3 and β-Ga_2O_3 are more selective than the other two oxides. For

Table 1
Reaction data in the absence of carbon dioxide

Catalyst	S_{BET} (m^2/g)	C_3H_8 conversion[a] (%)	Selectivity[a] (%)				Activity[a] ($\mu mol/(h\,m^2)$)
			C_3H_6	CH_4	C_2H_4	C_2H_6	
α-Ga_2O_3	72	25 (13)	96 (96)	1.5 (1.5)	2.9 (2.6)	0.0 (0.0)	12 (6.0)
β-Ga_2O_3	40	33 (12)	95 (95)	1.7 (1.0)	2.5 (2.7)	1.0 (1.6)	28 (10)
γ-Ga_2O_3	123	44 (18)	87 (95)	4.6 (2.4)	4.9 (2.9)	3.9 (0.0)	12 (4.8)
δ-Ga_2O_3	80	26 (9.3)	88 (95)	3.5 (1.8)	8.7 (3.7)	0.0 (0.0)	11 (4.0)
Cr_2O_3	4.8	5.2 (2.8)	91 (100)	8.7 (0.0)	0.0 (0.0)	0.0 (0.0)	36 (19)

[a] The values outside and inside the bracket are the data obtained in the initial period and at 6 h, respectively.

Table 2
Reaction data in the presence of carbon dioxide

Catalyst	S_{BET} (m^2/g)	Conversion[a] (%)		Selectivity[a] (%)				Activity[a] ($\mu mol/(h\,m^2)$)
		C_3H_8	CO_2	C_3H_6	CH_4	C_2H_4	C_2H_6	
α-Ga_2O_3	72	16 (9.7)	4.3 (3.4)	89 (94)	3.4 (1.7)	7.4 (3.1)	0.0 (1.4)	7.7 (4.6)
β-Ga_2O_3	40	23 (11)	6.2 (5.5)	94 (98)	2.3 (1.2)	3.1 (1.2)	0.3 (0.0)	20 (9.2)
γ-Ga_2O_3	123	21 (14)	4.4 (3.8)	86 (94)	5.4 (1.8)	7.9 (2.7)	0.0 (1.3)	5.7 (3.7)
δ-Ga_2O_3	80	18 (7.8)	5.3 (2.6)	93 (95)	2.6 (1.9)	4.0 (3.6)	0.0 (0.0)	7.5 (3.3)
Cr_2O_3	4.8	1.5 (0.8)	3.4 (2.7)	90 (100)	10 (0.0)	0.0 (0.0)	0.0 (0.0)	10 (5.6)

[a] The values outside and inside the bracket are the data obtained in the initial period and at 6 h, respectively.

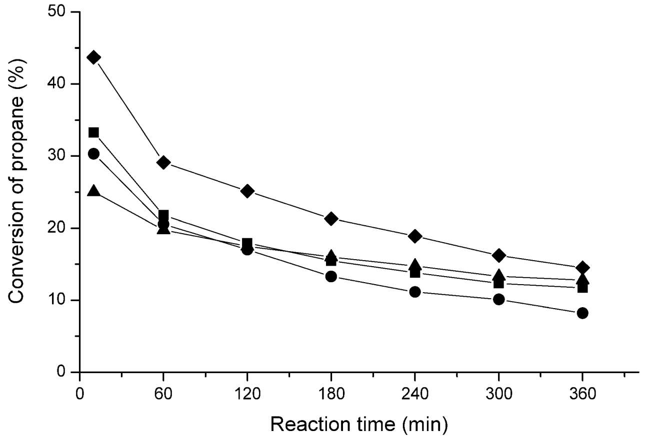

Fig. 2. Conversion of propane over four polymorphs of gallium oxide in the absence of carbon dioxide. ▲: α-Ga_2O_3; ■: β-Ga_2O_3; ◆: γ-Ga_2O_3; ●: δ-Ga_2O_3.

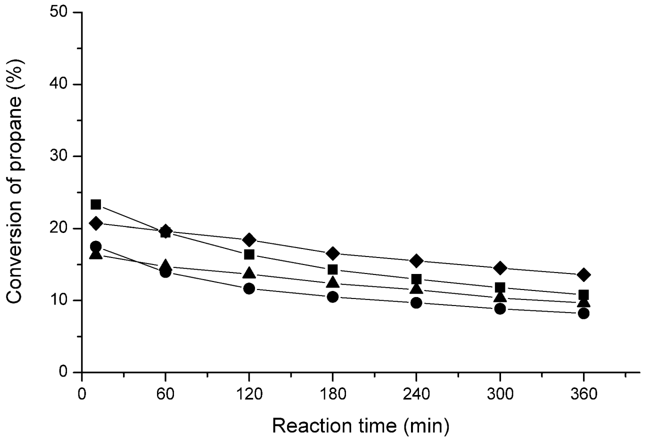

Fig. 3. Conversion of propane over four polymorphs of gallium oxide in the presence of carbon dioxide. ▲: α-Ga_2O_3; ■: β-Ga_2O_3; ◆: γ-Ga_2O_3; ●: δ-Ga_2O_3.

all of the catalysts, the selectivity for propene reaches 95% at steady state.

The propane dehydrogenation reaction was run on chromium oxide catalyst under the same conditions; the data are listed in Table 1 for comparison. It seems that the specific activity of chromium oxide is higher than that of β-Ga_2O_3 in the absence of CO_2.

3.3. Dehydrogenation of propane in the presence of CO_2

The dehydrogenation of propane was run over the gallium oxide catalysts in the presence of CO_2 at 500 °C; the reaction data are shown in Table 2 and Fig. 3. CO was detected in the reaction product. Again, the gallium oxides behave differently in the reaction. For all of the catalysts the initial conversion of propane is reduced in the presence of CO_2, but the catalysts are more stable with respect to reaction time. The propane conversions of the catalysts at steady state in the presence of CO_2 are only slightly lower than those in the absence of CO_2, and the activity order of the gallium oxides is unchanged. β-Ga_2O_3 remains intrinsically two to three times more active than the other types of gallium oxide. In the meantime, the selectivity for propene is also improved on β-Ga_2O_3 in the presence of CO_2. It can be as high as 97.6% at steady state. Moreover, in comparison with chromium oxide, β-Ga_2O_3 is more active for the reaction in the presence of CO_2. Its specific activity is almost twice as great as that of chromium oxide.

The gallium oxide catalysts after reaction for 6 h in the presence of CO_2 were studied by means of XRD, TGA, and N_2 adsorption methods. Fig. 4 illustrates the XRD patterns of the used catalysts, which are similar to those of the

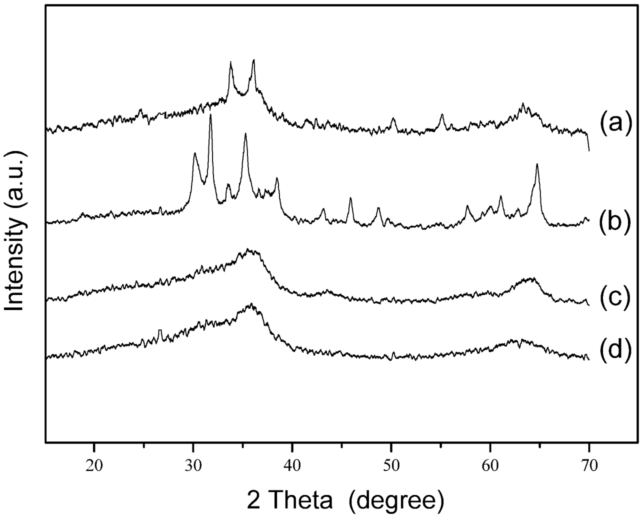

Fig. 4. XRD patterns of catalysts (a) α-Ga_2O_3; (b) β-Ga_2O_3; (c) γ-Ga_2O_3; (d) δ-Ga_2O_3 after 6 h of reaction in the presence of carbon dioxide at 500 °C.

Table 3
The amount of coke deposit and specific surface area of catalysts after 6 h reaction in the presence of CO_2

Catalyst	Amount of coke (%)	S_{BET} (m^2/g)
α-Ga_2O_3	4.18	51
β-Ga_2O_3	3.29	30
γ-Ga_2O_3	4.50	73
δ-Ga_2O_3	5.36	53
β-Ga_2O_3[a]	3.75	26

[a] The amount of coke and surface area of the catalyst after 6 h reaction in the absence of CO_2.

fresh catalysts, confirming the absence of structural change of the oxides during reaction. The amount of coke deposited on the catalysts measured by TGA and the specific surface areas of the catalysts after reaction are listed in Table 3. The low surface area of β-Ga_2O_3 probably accounts for the lower amount of coke deposited. In the absence of CO_2, the amount of coke deposited on β-Ga_2O_3 is obviously increased, and the reduction in surface area after reaction is more evident.

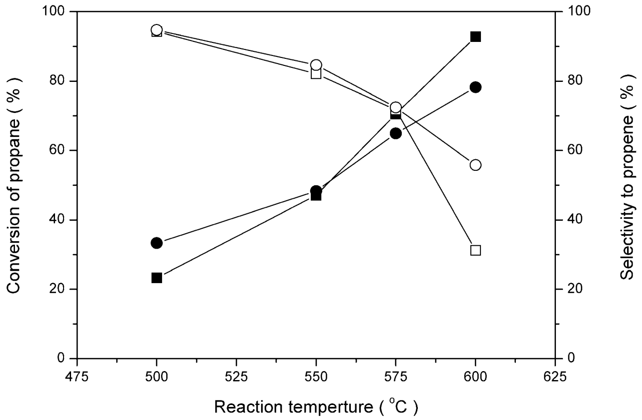

Fig. 5. Effect of reaction temperature on dehydrogenation of propane over β-Ga_2O_3 catalyst. ■: initial propane conversion in the presence of CO_2; □: initial propene selectivity in the presence of CO_2; ●: initial propane conversion in the absence of CO_2; ○: initial propene selectivity in the absence of CO_2.

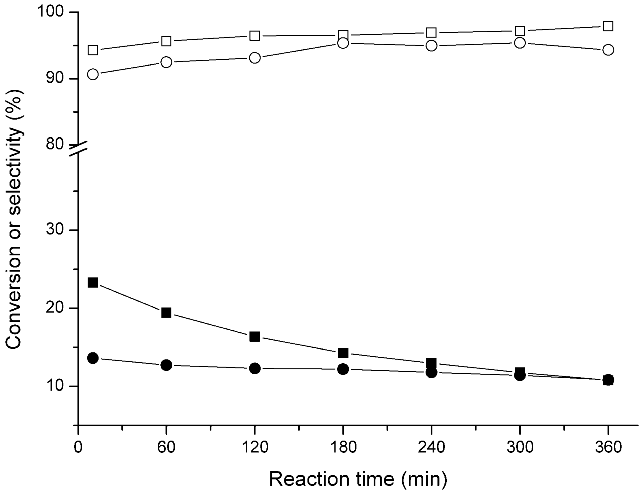

Fig. 6. Effect of pretreatment atmosphere on dehydrogenation of propane over β-Ga_2O_3 catalyst in the presence of CO_2. ■: propane conversion over β-Ga_2O_3 pretreated in N_2; □: propene selectivity over β-Ga_2O_3 pretreated in N_2; ●: propane conversion over β-Ga_2O_3 pretreated in H_2; ○: propene selectivity over β-Ga_2O_3 pretreated in H_2.

3.4. *Effect of reaction conditions*

Among the gallium oxides, β-Ga_2O_3 is the most stable one, and it can exist above 500 °C; so the effect of reaction temperature on dehydrogenation of propane over β-Ga_2O_3 in the presence or absence of CO_2 was studied. The reaction results are given in Fig. 5. At 500 °C, the initial conversion of propane in the presence of CO_2 is lower. However, it increases more steeply with temperature, so above 550 °C it starts to surpass the initial conversion of propane in the absence of CO_2, implying that the activation of CO_2 is favored at higher reaction temperatures. In both cases, the selectivity for propene is reduced as the reaction temperature is increased, but the reduction is more significant in the presence of CO_2.

The β-Ga_2O_3 catalyst was pretreated either in N_2 or in H_2 at 500 °C for 1 h before reaction. The effect of the pretreatment atmosphere on the dehydrogenation of propane in the presence of CO_2 was studied; the results are shown in Fig. 6. The initial propane conversion is decreased from 23.3 to 13.6% after H_2 pretreatment, but the catalyst becomes more stable. After 6 h of reaction, the propane conversion on the catalyst pretreated in H_2 becomes the same as that on the catalyst pretreated in N_2. In the meantime, the selectivity for propene on the catalyst pretreated in H_2 is slightly lower than that on the catalyst pretreated in N_2 during the whole course of reaction.

A regeneration treatment of the β-Ga_2O_3 catalyst after 6 h of reaction at 500 °C in the presence of CO_2 was at-

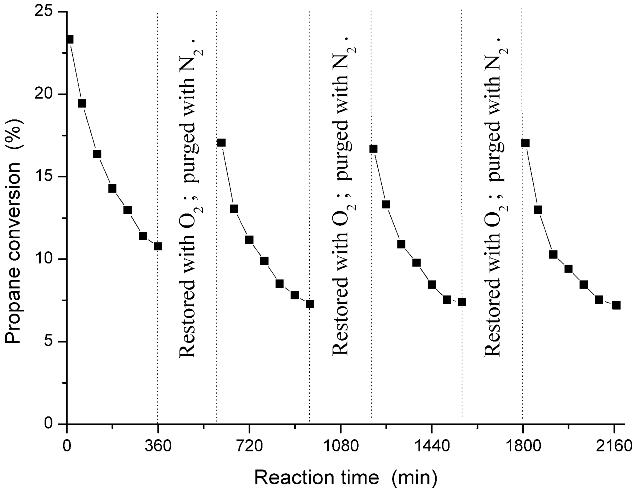

Fig. 7. Regeneration of β-Ga_2O_3 catalyst at 500 °C.

tempted. As shown in Fig. 7, the propane conversion on β-Ga_2O_3 catalyst decreases from 23.3 to 10.8% after 6 h on stream. The reaction was interrupted under a N_2 stream, and then O_2 was introduced at 500 °C for 1 h to burn off carbon species deposited on the catalyst. The propane conversion on the regenerated catalyst is 17.0%, which is much lower than the initial conversion, showing that the original activity of the catalyst could not be fully restored. Meanwhile, after the second and third regeneration, the activity of the catalyst is almost fully recovered. The increase in the activity after regeneration is due to the removal of carbonaceous deposits on the catalyst, and the reduction in the activity after the first regeneration could be due to the loss of some temporary active sites on the fresh catalyst.

3.5. *Acid–base properties*

The surface acidity of the four polymorphs of gallium oxide was measured by the NH_3-TPD method. A broad asymmetric NH_3 desorption peak is observed in the TPD profiles of all four samples. The peak temperatures are in the range of 300–400 °C, corresponding to acid sites of medium strength. NH_3-TPD data for the samples are listed in Table 4. The acid site density of the oxides (expressed in terms of $\mu mol/m^2$) has the sequence β-Ga_2O_3 > γ-Ga_2O_3 > δ-Ga_2O_3 > α-Ga_2O_3.

The surface basicity of the oxides was measured by the CO_2-TPD method, and the CO_2-TPD data were summarized in Table 5. Again, a low, broad, asymmetric CO_2 desorption peak is observed in the TPD profile of α-Ga_2O_3, β-Ga_2O_3, and γ-Ga_2O_3. The total amount of basic sites on the catalysts is 10 times lower than that of the acidic sites. The peak temperature of β-Ga_2O_3 is much lower than those of the others, demonstrating that the strength of the basic sites on β-Ga_2O_3 is much weaker. Furthermore, there are two distinct CO_2 desorption peaks on the TPD profile of δ-Ga_2O_3 with peak temperatures of 290 and 455 °C, respectively, showing the existence of a small amount of strong basic sites on the sample.

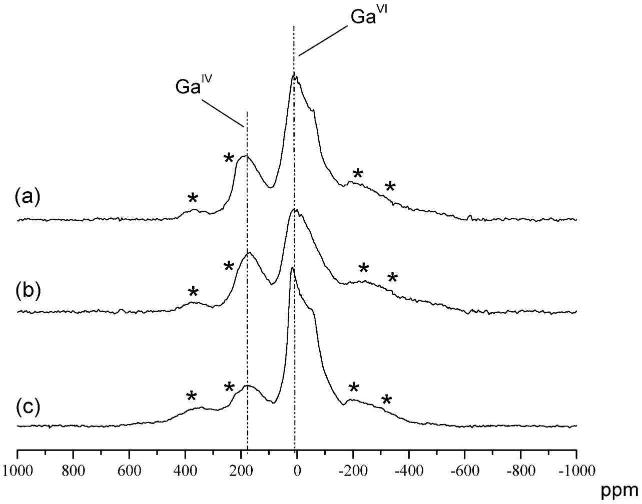

Fig. 8. ^{71}Ga MAS NMR spectra of gallium oxides. (a) β-Ga_2O_3; (b) γ-Ga_2O_3; (c) α-Ga_2O_3. Asterisks denote spinning sidebands.

The above measurements indicate that the gallium oxides are principally acidic oxides with medium acid strength. Only a negligible amount of basic sites exists on the oxides, implying that the acidic sites may play a more important role in the competition among the gallium oxides.

3.6. *^{71}Ga MAS NMR spectroscopy*

The ^{71}Ga MAS NMR chemical shift is known to reflect the coordination state of the Ga^{3+} ion in oxide compounds [19]. Fig. 8 shows the ^{71}Ga MAS NMR spectra of the polymorphs of gallium oxide. The spectra of β- and γ-Ga_2O_3 are composed of two main lines with maxima at 5–11 and 165–172 ppm, which are characteristic of gallium in sixfold (Ga^{VI}) and fourfold (Ga^{IV}) coordination to oxygen, respectively. The line attributed to Ga^{VI} splits into four spinning sidebands. The spectrum of α-Ga_2O_3 exhibits

Table 4
NH_3-TPD data of gallium oxide catalysts

Catalyst	Peak temperature (°C)	NH_3 desorbed	
		$mmol/g_{cat}$	$\mu mol/m^2_{cat}$
α-Ga_2O_3	360	0.54	7.6
β-Ga_2O_3	355	0.51	12.8
γ-Ga_2O_3	305	1.07	8.7
δ-Ga_2O_3	380	0.64	8.1

Table 5
CO_2-TPD data of gallium oxide catalysts

Catalyst	Peak temperature (°C)	CO_2 desorbed	
		$mmol/g_{cat}$	$\mu mol/m^2_{cat}$
α-Ga_2O_3	320	0.028	0.39
β-Ga_2O_3	240	0.022	0.55
γ-Ga_2O_3	365	0.023	0.17
δ-Ga_2O_3	290, 455	0.012	0.17

a strong asymmetric Ga^{VI} line and relatively weak evidence of the presence of tetrahedral Ga^{IV}, suggested by the small overlapped peak around 180 ppm. According to the published crystallographic data obtained by single crystal three-dimensional X-ray diffraction [20,21], α-Ga_2O_3 has a corundum structure containing only octahedral Ga ions, whereas β- and γ-Ga_2O_3 have both tetrahedral and octahedral Ga ions. The NMR result shows that the α-Ga_2O_3 in the present study is not strictly a single-phase compound. There is some tetrahedral Ga^{IV} species in the sample.

3.7. *TPR and XPS studies*

It has been reported that pure gallium oxide cannot be reduced by hydrogen below 600 °C [22,23]. Only when β-Ga_2O_3 is loaded onto zeolites, such as ultrastable faujasite and ZSM-5, is it amenable to reduction by H_2 [22,24]. The reducibility of the four polymorphs of gallium oxide was studied by H_2-TPR; the results are shown in Fig. 9 and Table 6. To our surprise, small reduction peaks appear in the TPR profiles of all of the samples above 200 °C, indicating that small parts of the gallium oxides can be reduced by H_2 at rather low temperature. Comparing our experimental conditions with those in the literature, it could be postulated that the omission of the reduction peak in the literature is caused by the low BET surface area (2.90 m^2/g) of the β-Ga_2O_3 used [23] or the low concentration of gallium oxide (1.7 mol%) [24] on the supported catalyst. Nevertheless, the amount of gallium oxide reduced by H_2 according to the TPR data is limited for all of the samples. After reduction the amount of low-valence gallium oxide in the sample is only about 1–5 mol%.

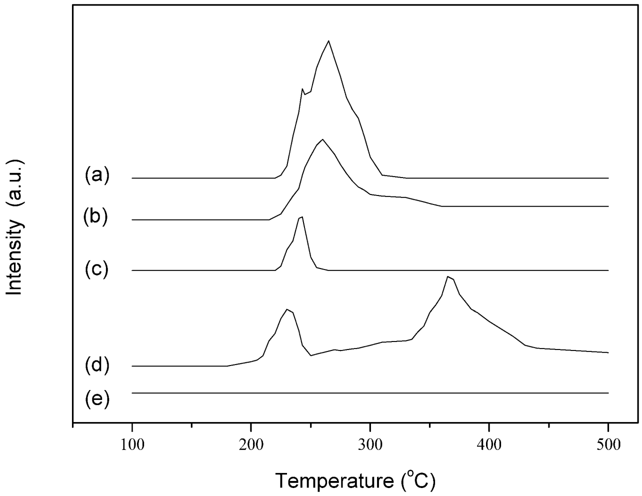

Fig. 9. H_2-TPR profiles of four polymorphs of gallium oxide. (a) α-Ga_2O_3; (b) β-Ga_2O_3; (c) γ-Ga_2O_3; (d) δ-Ga_2O_3; (e) O_2 regenerated β-Ga_2O_3 at 500 °C for 1 h after 6 h reaction in the presence of CO_2.

Table 6
H_2-TPR data of gallium oxide catalysts

Catalyst	Peak temperature (°C)	H_2 consumption	
		$mol/mol_{Ga_2O_3}$	$\mu mol/m^2_{cat}$
α-Ga_2O_3	265	0.10	7.7
β-Ga_2O_3	260	0.045	6.0
γ-Ga_2O_3	241	0.019	0.84
δ-Ga_2O_3	230, 366	0.083	5.6
β-Ga_2O_3[a]	–	0	0

[a] O_2 regenerated β-Ga_2O_3 at 500 °C for 1 h after 6 h reaction in the presence of CO_2.

It is more interesting to note that the O_2-regenerated β-Ga_2O_3 catalyst, after 6 h of reaction in the presence of CO_2, is not reduced by H_2 in TPR measurements, as shown in Fig. 9, indicating that the part of the reducible gallium oxide species in the catalyst is not restored after regeneration.

To confirm the valence change of gallium after reduction by H_2, the XPS spectra for β-Ga_2O_3 were recorded before and after reduction. The deconvoluted spectra in the Ga (3d) region appear in Fig. 10. Only two peaks appear in the spectrum of β-Ga_2O_3 at 25.0 and 20.8 eV, respectively, which can be assigned to O(2s) and Ga^{3+}(3d) bands, according to the literature [25]. A new small peak appears in the spectrum of β-Ga_2O_3 at 19.6 eV after reduction by H_2 at 500 °C for 1 h. This shift in binding energy (∼1.2 eV) can be attributed to the presence of $Ga_2{}^{+}O$ species in the reduced sample. From the ratio of the area of peak C to the total peak area,

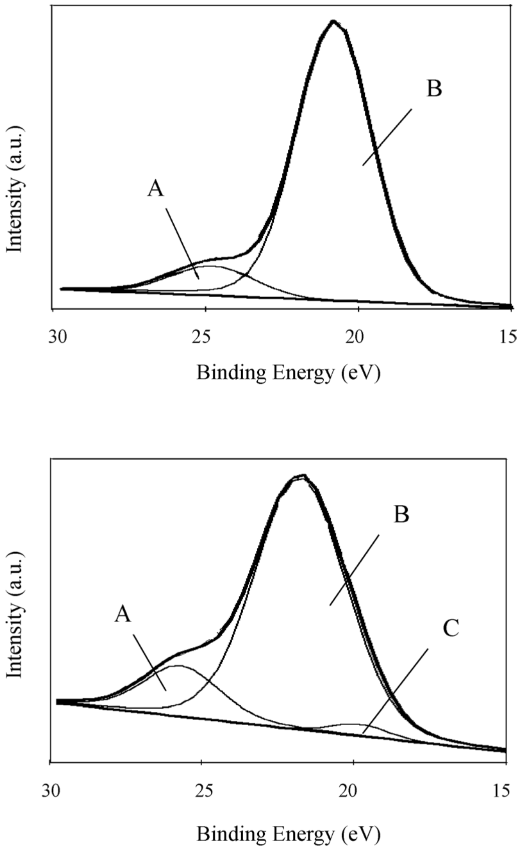

Fig. 10. XPS spectra of β-Ga_2O_3 before (top) and after reduction (bottom). (A) O(2s) signal peak; (B) Ga^{3+}(3d) signal peak; (C) Ga^{+}(3d) signal peak.

the amount of Ga^{3+} reduced to Ga^{+} can be calculated. The calculated value shows that about 2.5 mol% of Ga_2O_3 is reduced, that is, 0.05 mol H_2 per mol of Ga_2O_3 is consumed during reduction. This result is in accord with the H_2-TPR data in Table 6.

4. Discussion

The dehydrogenation of propane or ethane over reducible metal oxide catalysts, such as chromium and iron oxides, in the presence of CO_2 has been suggested to follow a redox mechanism [26,27]. Propane is oxidized to propene with the simultaneous reduction of metal oxide (Fe_2O_3, Cr_2O_3, and, etc.), and subsequently the reduced metal oxide catalyst is reoxidized by CO_2. Since gallium oxide is hardly reduced and the redox cycle is irreverible under the reaction temperature according to the experimental results in this work, the redox mechanism is probably inapplicable for the reaction. Previous studies have shown that the dihydrogen molecule is dissociatively adsorbed on gallium oxide, leading to the formation of H^- and H^+ ions [28]. Hence it has also been suggested [29] that propane can heterolytically dissociate on gallium oxide, forming gallium hydride and gallium alkoxide species:

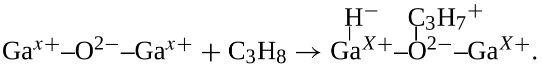
$$Ga^{x+}\text{–}O^{2-}\text{–}Ga^{x+} + C_3H_8 \rightarrow \overset{H^-}{Ga}{}^{X+}\text{–}\overset{C_3H_7^+}{O}{}^{2-}\text{–}Ga^{X+}. \qquad (1)$$

The alkoxides would decompose further to form the dehydrogenation products:

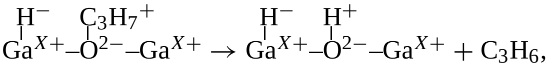
$$\overset{H^-}{Ga}{}^{X+}\text{–}\overset{C_3H_7^+}{O}{}^{2-}\text{–}Ga^{X+} \rightarrow \overset{H^-}{Ga}{}^{X+}\text{–}\overset{H^+}{O}{}^{2-}\text{–}Ga^{X+} + C_3H_6, \qquad (2)$$

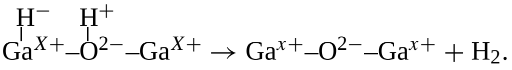
$$\overset{H^-}{Ga}{}^{X+}\text{–}\overset{H^+}{O}{}^{2-}\text{–}Ga^{X+} \rightarrow Ga^{x+}\text{–}O^{2-}\text{–}Ga^{x+} + H_2. \qquad (3)$$

Reaction (2) is slow and is the limiting step in the formation of propene [29]. When both Ga_2O_3 and H^+ are present on the catalyst, the propyl carbenium ion on Ga_2O_3 will readily exchange with a proton through a surface migration reaction:

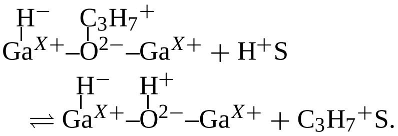
$$\overset{H^-}{Ga}{}^{X+}\text{–}\overset{C_3H_7^+}{O}{}^{2-}\text{–}Ga^{X+} + H^+S \rightleftharpoons \overset{H^-}{Ga}{}^{X+}\text{–}\overset{H^+}{O}{}^{2-}\text{–}Ga^{X+} + C_3H_7^+S. \qquad (4)$$

Propene then results from the equilibrium:

$$C_3H_7^+S \rightleftharpoons C_3H_6 + H^+S. \qquad (5)$$

The conjugated effect of gallium oxide and a proton is to replace the slow step (2) with the fast equilibrium (4).

NH_3-TPD studies of the polymorphs of gallium oxide show that acid sites of medium strength are abundant on the surface of these catalysts, particularly β-Ga_2O_3. The above reaction mechanism gives a good explanation not only for the high activity of the gallium oxide catalysts toward the dehydrogenation reaction, but also for the superiority of β-Ga_2O_3 over the other polymorphs.

Based on the analogy of gallium oxide to aluminum oxide, these acid sites should be the Lewis acid sites formed via abstraction of OH groups from gallium cations in tetrahedral positions [30]. It is known that tetrahedral Ga ions exist in the structure of β- and γ-Ga_2O_3, and surely they are the source of the Lewis acidity. By contrast, α- and δ-Ga_2O_3 are constituted only by octahedral Ga^{3+}, and theoretically the formation of Lewis acid sites on these oxides is unlikely. However, the results in Table 4 show that the surface acidities of γ-, α-, and δ-Ga_2O_3 are similar when normalized to unit surface area. Recently, other authors have also reported that γ- and α-Ga_2O_3 have nearly the same surface acidity, according to IR spectroscopic results obtained with CO and pyridine as probes [19]. This unexpected phenomenon was interpreted in the literature [19] as the occurrence of some surface reconstruction in α-Ga_2O_3, giving rise to tetrahedral Ga^{IV} species from bulk octahedral Ga^{VI}, because there is a high preference for tetrahedral versus octahedral coordination in the presence of d^{10} Ga^{3+} cations due to an enhanced polarizing power. The small peak around 180 ppm in the ^{71}Ga NMR spectrum of α-Ga_2O_3 in Fig. 8 confirms that a small number of tetrahedral Ga^{IV} ions are present in our α-Ga_2O_3 sample. More importantly, these Ga^{IV} ions formed by surface reconstruction are situated on the surface of the sample, and they are all accessible to the reactant and probe molecules.

When the reactivity of the polymorphs is correlated with the results of acidity measurements, it can be concluded that the surface acid site density probably plays a decisive role in the competition between the polymorphs. β-Ga_2O_3 is the most active catalyst because it has the highest surface acid site density (see Table 4), whereas the activities of the other three polymorphs are similar but lower, because of their reduced surface acid site density.

There is only a very small amount of surface basic sites on the oxide polymorphs. TPD experiments show that the surface basic site density is about 20 times lower than the surface acid site density. The low basicity and, consequently, the weak adsorption of CO_2 are probably correlated with the low conversion of CO_2. An appropriate enhancement of the catalyst surface basicity could be useful for the reaction, and this merits further study.

TPR and XPS results show that about 1–5 mol% of the fresh gallium oxide catalysts can be reduced below 500 °C, but this part of the reducible oxide cannot be restored after reaction and O_2 regeneration. If we correlate these results with the regeneration pattern of the used catalysts in Fig. 7, it could be postulated that the redox cycle between Ga^{3+} and Ga^{+} in the initial stage of the reaction might be of advantage to the dehydrogenation reaction. Nevertheless, the above observation still must be confirmed by more careful and precise measurements.

As regards the promoting effect of CO_2, the reverse water gas shift reaction (6) and the Boudouard reaction (7) may play positive roles in the dehydrogenation reaction:

$$CO_2 + H_2 \rightarrow CO + H_2O, \qquad (6)$$

$$C + CO_2 \rightarrow CO. \qquad (7)$$

Reaction (6) transforms H_2 with CO_2 into CO and H_2O and shifts the reactions (2), (3), and (4) to the product side, leading to the enhancement of the total reaction rate. Meanwhile, reaction (7) removes the carbon deposit from the catalyst surface and improves the stability of the catalyst. The CO in the reaction products is associated with these reactions.

In the literatures [11–14], the promoting effect of CO_2 on the dehydrogenation of propane or ethane over gallium oxide catalysts was often tested at 600–700 °C. Under these temperatures, gallium oxide was found to be more effective for the reaction, and the yield of olefin was increased more evidently in the presence of CO_2. The aim of the present work is to investigate and compare the catalytic performance of different polymorphs of gallium oxide in the reaction. Because of the instability of some of the polymorphs at high temperature, the dehydrogenation reaction temperature was set at 500 °C. Experimental results at such a low temperature show that the promoting effect of CO_2 is relatively less significant, particularly at the initial stage of reaction. To make up for this inadequacy, the reaction was run over β-Ga_2O_3 under different temperatures (Fig. 5). The propane conversion increases significantly above 550 °C, in particular, in the presence of CO_2, demonstrating that β-Ga_2O_3 is probably the most practical polymorphic form for this type of reaction.

5. Conclusions

Dehydrogenation of propane over different polymorphs of gallium oxide in the presence or absence of CO_2 was studied. Among the polymorphs, β-Ga_2O_3 exhibits the highest dehydrogenation activity, in both the presence and absence of CO_2. It is even more active than chromium oxide in the presence of CO_2. H_2-TPR and XPS studies show that gallium oxide is hardly reduced (< 5 mol%) below 600 °C, and the reduced gallium oxide is not restored after O_2 regeneration. Thus, the dehydrogenation of C_3H_8 occurs on gallium oxide, probably through a heterolytic dissociation reaction pathway instead of a redox mechanism. The reverse water gas shift reaction and the Boudouard reaction of CO_2 account for the enhanced catalytic activity and stability in the presence of CO_2. NH_3-TPD measurement shows that the surface acid site density of β-Ga_2O_3 is the highest among all of the polymorphs, which facilitates the conjugated effect of protons and oxide and promotes the reaction. ^{71}Ga MAS NMR spectroscopic studies suggest that the surface acidity of the gallium oxides is related to the presence of tetracoordinated Ga^{IV} ions.

Acknowledgments

This work was supported by the Chinese Major State Basic Research Development Program (grant no. 2000077507), the National Natural Science Foundation of China (grant no. 20303004), the Shanghai Major Basic Research Program (grant no. 03DJ14004), and the Shanghai Natural Science Foundation (grant no. 03ZR14013). The authors thank Prof. Heyong He, Mr. Tailiu Wu, and Mr. Liping Wang for their assistance with the NMR measurement.

References

[1] I. Takahara, M. Saito, Chem. Lett. (1996) 973.
[2] I. Takahara, W.C. Chang, N. Mimura, M. Saito, Catal. Today 45 (1998) 55.
[3] B. Zhaorigetu, R. Kieffer, J.P. Hindermann, Stud. Surf. Sci. Catal. 101 (1996) 1049.
[4] P. Michorczyk, J. Ogonowski, React. Kinet. Catal. Lett. 78 (2003) 41.
[5] P. Mériaudeau, C. Naccache, J. Mol. Catal. 50 (1989) L7.
[6] P. Schulz, M. Baern, Appl. Catal. 78 (1991) 15.
[7] M. Guisnet, N.S. Gnep, F. Alaris, Appl. Catal. A 89 (1992) 1.
[8] Y. Ono, Catal. Rev. Sci. Eng. 34 (1992) 179.
[9] B.S. Kwak, W.M.H. Sachtler, J. Catal. 145 (1994) 456.
[10] P. Mériaudeau, C. Naccache, Catal. Today 31 (1996) 265.
[11] K. Nakagawa, M. Okamura, N. Ikenaga, T. Suzuku, T. Kobayashi, Chem. Commun. (1998) 1025.
[12] K. Nakagawa, C. Kajita, Y. Ide, M. Okamura, S. Kato, H. Kasuya, N. Ikenaga, T. Kobayashi, T. Suzuki, Catal. Lett. 64 (2000) 215.
[13] K. Nakagawa, C. Kajita, K. Okumura, N. Ikenaga, M. Nishitani-Gamo, T. Ando, T. Kobayashi, T. Suzuki, J. Catal. 203 (2001) 87.
[14] P. Michorczyk, J. Ogonowski, Appl. Catal. A 251 (2003) 425.
[15] R. Roy, V.G. Hill, E.F. Osborn, J. Am. Chem. Soc. 74 (1952) 719.
[16] C.O. Areán, A.L. Bellan, M.P. Mentruit, M.R. Delgado, G.T. Palomino, Micropor. Mesopor. Mater. 40 (2000) 35.
[17] M.R. Delgado, C.O. Areán, Mater. Lett. 57 (2003) 2292–2297.
[18] J. Böhm, Angew. Chem. 53 (1940) 131.
[19] J.C. Lavalley, M. Daturi, V. Montouillout, G. Clet, C.O. Areán, M.R. Delgado, A. Sahibed-dine, Phys. Chem. Chem. Phys. 5 (2003) 1301.
[20] S. Geller, J. Chem. Phys. 33 (1960) 676.
[21] M. Marezio, J.P. Remeika, J. Chem. Phys. 46 (1967) 1862.
[22] B. Sulikowski, Z. Olejniczak, V.C. Corberán, J. Phys. Chem. 100 (1996) 10323.
[23] M. Saito, S. Watanabe, I. Takahara, M. Inaba, K. Murata, Catal. Lett. 3–4 (2003) 213.
[24] G.L. Price, V. Kanazirev, J. Catal. 126 (1990) 267.
[25] R. Carli, C.L. Bianchi, R. Giannantonio, V. Ragaini, J. Mol. Catal. 83 (1993) 379.
[26] S.B. Wang, K. Murata, T. Hayakawa, S. Hamakawa, K. Suzuki, Appl. Catal. A 196 (1998) 1.
[27] P. Michorczyk, P. Kuśtrowski, L. Chmielarz, J. Ogonowski, React. Kinet. Catal. Lett. 82 (2004) 121.
[28] P. Meriaudeau, M. Primet, J. Mol. Catal. 61 (1990) 227.
[29] P. Meriaudeau, C. Naccache, J. Mol. Catal. 59 (1990) L31.
[30] O.O. Parengo, Yu.N. Pushkar, A.O. Turakulova, G.P. Murav'eva, E.V. Lunina, Kinet. Catal. 39 (1998) 288.